communications medicine

A Nature Portfolio journal

Article

https://doi.org/10.1038/s43856-025-01152-7

The metformin mediated MAPK signaling pathway influences D-Xylose regulation during diabetic kidney disease therapy

Dandan Xie[1,3], Yongjun Zhu[1,3], Sifan Guo[1,3], Hao Li[1,3], Zhibo Wang[1], Xian Wang[1], Ying Cai[1,2], Jinxuan Chai[1], Yan Wang[1], Zhencai Hu[1], Shiwei Wang[1], Lasi Chen[1] ✉, Shi Qiu[1] ✉, Yiqiang Xie[1] ✉ & Aihua Zhang[1,2] ✉

Abstract

Background: Diabetic kidney disease (DKD) is a major cause of end-stage renal disease. Although metformin is widely prescribed, the mechanisms underlying its renoprotective effects remain incompletely understood.

Methods: We integrated multi-omics approaches—including network pharmacology, phosphoproteomics, and targeted metabolomics—in both db/db mice (male) and human patients. Analyses were performed on blood and kidney tissue from mice and paired blood/urine samples from DKD patients to identify conserved therapeutic targets and metabolic pathways.

Results: Metformin treatment improves glycemic control and renal function (reduced creatinine and urea nitrogen) in DKD mice. Network pharmacology and phosphoproteomic analyses reveal metformin's engagement with the MAPK pathway, specifically through MAPK1 and MAPK3. Targeted metabolomics identifies four carbohydrate metabolites (mannitol, D-arabitol, D-mannose, and D-xylose) associated with DKD risk in humans. Cross-species validation in mice supports D-Xylose as a potential key biomarker for metformin's therapeutic effects in DKD, with proximal tubule bicarbonate reclamation and alanine, aspartate and glutamate metabolism as key metabolic pathways.

Conclusions: Metformin alleviates DKD through multi-modal mechanisms, modulating the MAPK signaling pathway and carbohydrate metabolites—notably D-xylose. As far as we are aware, these findings provide new mechanistic insights and suggest potential biomarker-driven strategies for DKD management.

Plain language summary

Diabetic kidney disease is a serious complication of diabetes in which the kidney becomes damaged. While metformin is a common medication used as a treatment, exactly how it impacts the kidneys is not fully clear. In this study, we analyzed samples from mice and humans with diabetic kidney disease. We found that metformin lowers blood sugar and alters the behavior of cells. These results help explain how metformin treatment can have a beneficial effect on kidney function and suggests new ways to monitor the effects of metformin on kidney function. Our findings may lead to more personalized strategies for managing diabetic kidney disease in the future.

The increasing incidence of diabetes mellitus (DM) due to an aging population and lifestyle changes has become a significant global public health issue. According to the International Diabetes Federation (IDF) Diabetes Atlas, the number of adults with DM is projected to rise from 537 million in 2021 to 783 million by 2045[1], up to 40% of these individuals are expected to develop chronic kidney disease (CKD)[2], known as diabetic kidney disease (DKD). DKD, characterized by persistent proteinuria and/or a progressive decline in glomerular filtration rate, is one of the most prevalent complications of DM and a leading cause of end-stage renal disease (ESRD)[3]. Type 2 diabetes mellitus (T2DM) is the primary contributor to the disease burden related to DKD[2]. Persistent hyperglycemia induces metabolic disturbances, leading to renal inflammation, oxidative stress, apoptosis, autophagy, and abnormal expression or activation of related signaling molecules and pathways, ultimately resulting in renal fibrosis and DKD[4].

Metformin is a cornerstone medication for controlling hyperglycemia, known for its efficacy, safety, and tolerability[5,6]. It also possesses multiple extraglycemic benefits, such as cardiovascular and renal protection. Several guidelines[7–9], including the American Diabetes Association (ADA), recommend metformin as the first-line hypoglycemic agent for patients with T2DM or DKD. Metformin ameliorates hyperglycemia by inhibiting

[1]International Advanced Functional Omics Platform, School of Chinese Medicine, Scientific Experiment Center, Public Research Center, Hainan Medical University, Haikou, China. [2]Graduate School, Heilongjiang University of Chinese Medicine, Harbin, China. [3]These authors contributed equally: Dandan Xie, Yongjun Zhu, Sifan Guo, Hao Li. ✉e-mail: 251849367@qq.com; qiushihnyx@163.com; xieyiqiang@hainmc.edu.cn; aihuatcm@163.com

hepatic gluconeogenesis, enhancing insulin sensitivity in peripheral tissues, and increasing intestinal glucose excretion[10]. Additionally, metformin has been shown to impact apoptosis, autophagy, and inflammation via the MAPK/ERK and AMPK-related signaling pathways, thereby improving energy metabolism in the liver, kidney, muscle, and fat to exert protective effects[11–13]. However, the precise mechanism and direct molecular targets of metformin in the treatment of DKD remain unknown.

Metabolomics, an emerging discipline following genomics and proteomics, utilizes mass spectrometry (MS) technology to qualitatively and quantitatively analyze metabolites in biological organisms through high-throughput methods[14,15]. This field primarily studies small molecules with molecular weights under 1500 Da, such as glucose, amino acids, and lipids. Analyzing metabolic changes and interactions of small molecule metabolites in pathophysiological processes can help identify disease-related biomarkers and elucidate potential mechanisms and metabolic networks for drug therapy[14,15].

Proteomics is the study of the proteome, focusing on the composition, expression levels, protein-protein interactions (PPI), and post-translational modifications (PTMs) of proteins under physiological and pathological conditions[16]. DNA is transcribed into mRNA and then translated into proteins with specific amino acid sequences to function in the body, most of which require chemical modification processes such as adding or removing specific amino acids or chemical functional groups (i.e., PTMs) to dynamically regulate protein function and stability[17]. Phosphorylation is one of the most prevalent types of PTMs, where the phosphoryl group at the γ-site of ATP or GTP is transferred to the amino acid residues of substrate proteins through the catalytic action of a protein kinase, modulating protein structure, activity, and PPI[18]. Phosphoproteomics, based on MS and high-throughput technologies, plays an important role in understanding metabolic pathways, disease development mechanisms and identifying therapeutic targets through the identification and quantitative analysis of phosphorylation sites[19].

In this study, the hypoglycemic and renal protective effects of metformin are confirmed in db/db mice, a model that recapitulates the key hallmarks of human type 2 DKD. Network pharmacology analysis, utilizing bioinformatics tools and systems biology, predicts potential targets and signal pathways of metformin treatment for DKD, suggesting a mechanism related to protein phosphorylation. Phosphoproteomics analysis of mouse kidneys identifies differentially phosphorylated proteins and modified sites, followed by functional enrichment analysis. KEGG annotation analysis suggests that differentially phosphorylated proteins are closely related to carbohydrate metabolism. Targeted carbohydrate metabolomics analysis of blood and urine from DKD patients identifies potential biomarkers, which are validated using mouse blood metabolomics. The combined analysis of network pharmacology, phosphoproteomics, metabolomics, and molecular docking verification suggests that MAPK1 and MAPK3 may represent potential targets for metformin treatment of DKD. The MAPK signaling pathway is identified as a potential signaling pathway, D-Xylose as a potential biomarker, and proximal tubule bicarbonate reclamation and alanine, aspartate, and glutamate metabolism as potential metabolic pathways. This study may contribute to a more comprehensive understanding of metformin's potential mechanisms in the treatment of DKD.

Methods

Materials and reagents

Metformin (Cat: H20023370) was purchased from Merck Pharmaceutical Co., Ltd. (Jiangsu, China). Carboxymethyl cellulose sodium (CMC-Na) (Cat: C14456738) was obtained from Shanghai Maclean Biochemical Technology Co., Ltd. (Shanghai, China). Blood glucose meter (GA-3) was acquired from Sinocare Biosensor Co., Ltd. (Hunan, China). Creatinine Assay kit (Cat: 20240530) and Urea Assay Kit (Cat: 20240530) were purchased from Nanjing Jiancheng Bioengineering Institute (Jiangsu, China).

Animals

Seven-week-old male C57BL/KsJ-db/db mice (db/db, 41.2 ± 1.1 g) and C57BL/KsJ-db/m mice (db/m, 20.0 ± 0.9 g) were procured from GemPharmatech Co., Ltd. (Jiangsu, China). Male mice were used to avoid the potential confounding effects of sex hormones and the estrous cycle on metabolic phenotypes and disease progression. All experimental animals were housed under standardized specific pathogen-free (SPF) conditions with environmental enrichment at the Animal Experimental Center of Hainan Medical University, with a temperature of 25 ± 2 °C, humidity of 65 ± 5%, and a 12 h light/12 h dark cycle, with free access to food and water. All procedures in this study were approved by the Ethics Committee of Hainan Medical University (Ethics No.: HYLL-2023-457) and adhered to the Guidelines for the Care and Use of Laboratory Animals published by the National Institutes of Health (NIH Publication No. 85-23, revised 1996).

Animal treatment

A total of 18 mice were used in this experiment. After a one-week acclimatization period, db/db mice with confirmed hyperglycemia (fasting blood glucose >11.1 mmol/l) and age-matched normoglycemic db/m mice were included. Mice were randomly assigned to three groups: db/db model group (Model), metformin-treated db/db group (MET), and control db/m group (Control), $n = 6$ per group, using a random number table generated prior to treatment allocation. Sample size was determined based on previous studies using db/db mice in DKD research and on feasibility considerations[20], sufficient to detect biologically meaningful differences while adhering to the principle of reduction in animal use. To minimize confounders, cage positions were rotated weekly and the order of treatment administration and sample collection was randomized. Investigators were blinded to group allocation during outcome assessment and data analysis. Metformin was administered at an equivalent dose of 65 mg/kg/d based on clinical dosing guidelines for DKD, while the control and model groups received equal volumes of 0.5% CMC-Na solution. Humane endpoints included >20% body weight loss within 48 h or inability to eat/drink. No adverse events or mortality occurred, and no animals required early euthanasia. All treatments were delivered via intragastric gavage for 4 weeks. Fasting blood glucose (FBG) levels in each group were measured using a blood glucose meter. At the end of the experiment, all mice were euthanized, and blood was collected. After centrifugation, the upper serum was collected and stored at −80 °C for subsequent metabolomics analyses. Serum creatinine (SCr) and blood urea nitrogen (BUN) levels in each group were determined according to the manufacturer's instructions. The left kidneys of mice in each group were frozen in liquid nitrogen-isopentane and stored in a −80 °C refrigerator for subsequent phosphoproteomics analysis. The right kidneys were fixed in 4% paraformaldehyde and stored at 4 °C for histopathological section preparation.

Renal tissue sections were cut for hematoxylin and eosin (H&E) and periodic acid-Schiff (PAS) staining. Evaluation of glomerular and tubular damage was performed on PAS-stained paraffin-embedded kidney sections in a double-blinded manner, as previously described[21–23]. Specifically, glomerular injury was semi-quantitatively graded on a scale of 0–4 based on the extent of mesangial matrix expansion, thickening of the glomerular basement membrane, and glomerulosclerosis. Tubulointerstitial injury was scored from 0 to 4 according to the severity of tubular epithelial cell damage, intraluminal cast formation, interstitial inflammation, and extracellular matrix accumulation.

Clinical study

A total of 14 participants were enrolled in this study at the First Affiliated Hospital of Hainan Medical University, comprising 7 DKD patients and 7 healthy controls. The detailed clinical characteristics of the participants are provided in supplementary materials (Supplementary Table 3). The study was approved by the Medical Ethics Committee of the First Affiliated Hospital of Hainan Medical University (2024-KYL-040). DKD Patients were diagnosed by clinicians based on the KDIGO 2022 Clinical Practice Guideline for Diabetes Management in CKD[9]. Healthy volunteers were recruited from the health examination center and were matched to DKD patients in a 1:1 ratio using propensity score matching based on age and sex. All healthy volunteers were confirmed to be free of DM or kidney disease.

All participants, both DKD patients and healthy individuals, had not been exposed to toxic substances within the past 3 months, had not used drugs harmful to the kidneys, and had signed informed consent forms. Blood and urine samples were collected from all participants for targeted metabolic profiling by ultra-high performance liquid chromatography (UPLC) and MS using a standardized metabolomics platform. Trial registration: Public title: The value of the combined omics technique in the early diagnosis of patients with DKD. Registration date: 26/12/2023. Registration number: ChiCTR2300079160. Registry URL: http://www.chictr.org.cn.

Network pharmacology analysis

The 3D structure and canonical SMILES of metformin were obtained from PubChem. Potential targets for metformin were identified using Swisstarget, TargetNet, Therapeutic Target Database (TTD), DrugBank, and ChEMBL databases. The corresponding gene names for the target proteins were retrieved from the UniProt database (https://www.uniprot.org/)."Diabetic Nephropathy" or "Diabetic Kidney Disease" were used as keywords to screen targets in the Online Mendelian Inheritance in Man (OMIM) database (http://www.omim.org/), Drugbank (https://go.drugbank.com/), GeneCards database (https://www.genecards.org), TTD and DisGeNET (https://www.disgenet.org/). The intersection of metformin targets and DKD disease targets was mapped to identify potential therapeutic targets. These potential targets were imported into the STRING database with species set to "Homo sapiens" and a confidence score threshold of > 0.4 to obtain PPI data. A PPI target network map was constructed using Cytoscape 3.10.1 software, selecting targets with a degree greater than the mean as core targets. Gene Ontology (GO) enrichment analysis and Kyoto Encyclopedia of Genes and Genomes (KEGG) pathway enrichment analysis for core targets of metformin treatment in DKD were performed using the Metascape data platform (https://metascape.org/gp/index.html) and the bioinformatics online tool (https://www.bioinformations.com.cn/).

Phosphorylated proteomics analysis

Lysis buffer (8 M urea, 1% protease inhibitor, 1% phosphatase inhibitor, 50 μM PR-619, 3 μM TSA, 50 mM NAM) was added to samples from each group, and ultrasonic lysis was performed, followed by centrifugation. The protein concentration in the supernatant was measured using a BCA kit. For trypsin digestion, 20% trichloroacetic acid was added to each sample, mixed by vortexing, centrifuged, and the precipitate was collected and dried. The 200 mM tetraethylammonium bromide was added and ultrasonically dispersed, and then digested with trypsin at a 1:50 mass ratio overnight. The reduction was carried out using 5 mM DL-dithiothreitol at 56 °C for 30 min, followed by alkylation with 11 mM iodoacetamide for 15 min at room temperature in the dark. Peptides were dissolved in an enrichment buffer (50% acetonitrile/0.5% acetic acid) and incubated with IMAC beads under shaking. The non-specifically adsorbed peptides were removed, elution buffer containing 10% NH4OH was added, and the collected eluate containing enriched phosphopeptides was lyophilized for LC-MS/MS analysis.

Enriched peptides were dissolved in solvent A and separated using a NanoElute ultra-high performance liquid system (Bruker Daltonics). Solvent A consisted of 0.1% formic acid and 2% acetonitrile in water, while solvent B contained 0.1% formic acid in acetonitrile. The liquid gradient was set as follows: 0–16 min, 2–22% B; 16–22 min, 22–35% B; 22–26 min, 35–90% B; 26–30 min, 90% B. The flow rate was maintained at 450 nl/min. Peptides were analyzed using the timsTOF Pro 2 mass spectrometry with a capillary source. The ion source voltage was set to 1.7 kV. Data acquisition was performed in the data-independent parallel accumulation serial fragmentation (dia-PASEF) mode. The full MS scan range was 100–1700 m/z, the MS/MS scan range was 395–1395 m/z, and the isolation window was set to 20 m/z.

Metabolomics analysis

Methanol was added to human or mouse samples, followed by centrifugation at 13,200 × *g* for 10 min at 4 °C. The supernatant was concentrated and dried, then reconstituted with 2-chloro-L-phenylalanine (4ppm) solution prepared in 80% methanol-water, finally filtered through a 0.22 μm microporous membrane for subsequent analysis.

Each sample group was analyzed using UPLC and MS. UPLC was performed on a Thermo Vanquish ultra-performance liquid system (Thermo Fisher Scientific, USA) using an ACQUITY UPLC®HSS T3 column (2.1 × 100 mm, 1.8 μm) (Waters, Milford, MA, USA) maintained at 40°C, with a flow rate of 0.3 mL/min and an injection volume of 2 μL. The mobile phase consisted of phase A (0.1% formic acid in water) and phase B (0.1% formic acid in acetonitrile). The gradient elution procedure was as follows: 0–1 min, 8% B; 1–8 min, 8–98% B; 8–10 min, 98% B; 10–10.1 min, 98-8% B; 10.1–12 min, 8% B.

MS was performed using a Thermo Orbitrap Exploris 120 mass spectrometer (Thermo Fisher Scientific, USA) with an electrospray ionization (ESI) source. The positive ion spray voltage was set to 3.50 kV, and the negative ion spray voltage was −2.50 kV. The sheath gas and auxiliary gas were set to 40 arb and 10 arb, respectively.

As described previously[24], raw mass spectrometry files were converted into the common data format (.mzXML) using the MSConvert tool from the Proteowizard software package (version 3.0.8789). Peak detection, filtering, and alignment of retention time (RT) and mass-to-charge ratio (m/z) were carried out using the R-based XCMS software package to generate a metabolite quantification list. Data normalization was performed through total peak area normalization to correct for systematic errors and enable reliable comparisons between samples and metabolites. Identification of secondary metabolites was achieved by matching exact mass values (<25 ppm) and conducting retrieval and comparison using spectral databases such as the Human Metabolome Database (http://www.hmdb.ca/), LipidMaps (http://www.lipidmaps.org/), MassBank (http://massbank.jp/), mzCloud (http://www.mzcloud.org/), and KEGG.

Molecular docking

CB-DOCK2, a semi-flexible molecular blind docking method based on a complex network, was used to evaluate the binding ability of protein and ligand according to comprehensive characteristics. CB-DOCK2 online molecular docking software facilitated the docking of potential DKD targets with metformin. The binding strength and activity between these targets and metformin were assessed based on binding energy.

Statistics and reproducibility

Continuous variables are presented as mean ± standard error of the mean (SEM), and categorical data as counts and proportions. Statistical analyses were performed using GraphPad Prism (v.10.1.2, San Diego, CA, USA). Normality and homogeneity of variances were assessed using the Shapiro–Wilk test and Brown–Forsythe test, respectively. For comparisons between two groups, an unpaired two-tailed Student's *t* test was used. For multiple comparisons, one-way analysis of variance (ANOVA) followed by Tukey's post-hoc test was applied. If data did not meet the assumptions of parametric tests, non-parametric alternatives (Mann–Whitney U test or Kruskal–Wallis test with Dunn's correction) were used. A $P < 0.05$ was considered statistically significant. The exact sample size (n) for each experiment is provided in the corresponding figure legend.

Results

Metformin exhibits hypoglycemic and renal protective effects in DKD

The efficacy of metformin on DKD was evaluated using a mouse model. Compared to the control group, the model group exhibited significantly elevated FBG ($P < 0.001$), SCr ($P < 0.001$), and BUN ($P < 0.001$), alongside a significantly reduced kidney index (KI; kidney weight/body weight; $P < 0.001$). Metformin treatment markedly reversed these pathological changes, resulting in significantly decreased FBG ($P < 0.001$), SCr ($P < 0.001$) and BUN ($P = 0.0013$) levels, as well as a significant increase in KI ($P = 0.0337$), when compared to untreated DKD mice (Fig. 1a–d).

Histopathological evaluation of kidney tissue sections using H&E staining and PAS staining, with representative images shown in Fig. 1e–h.

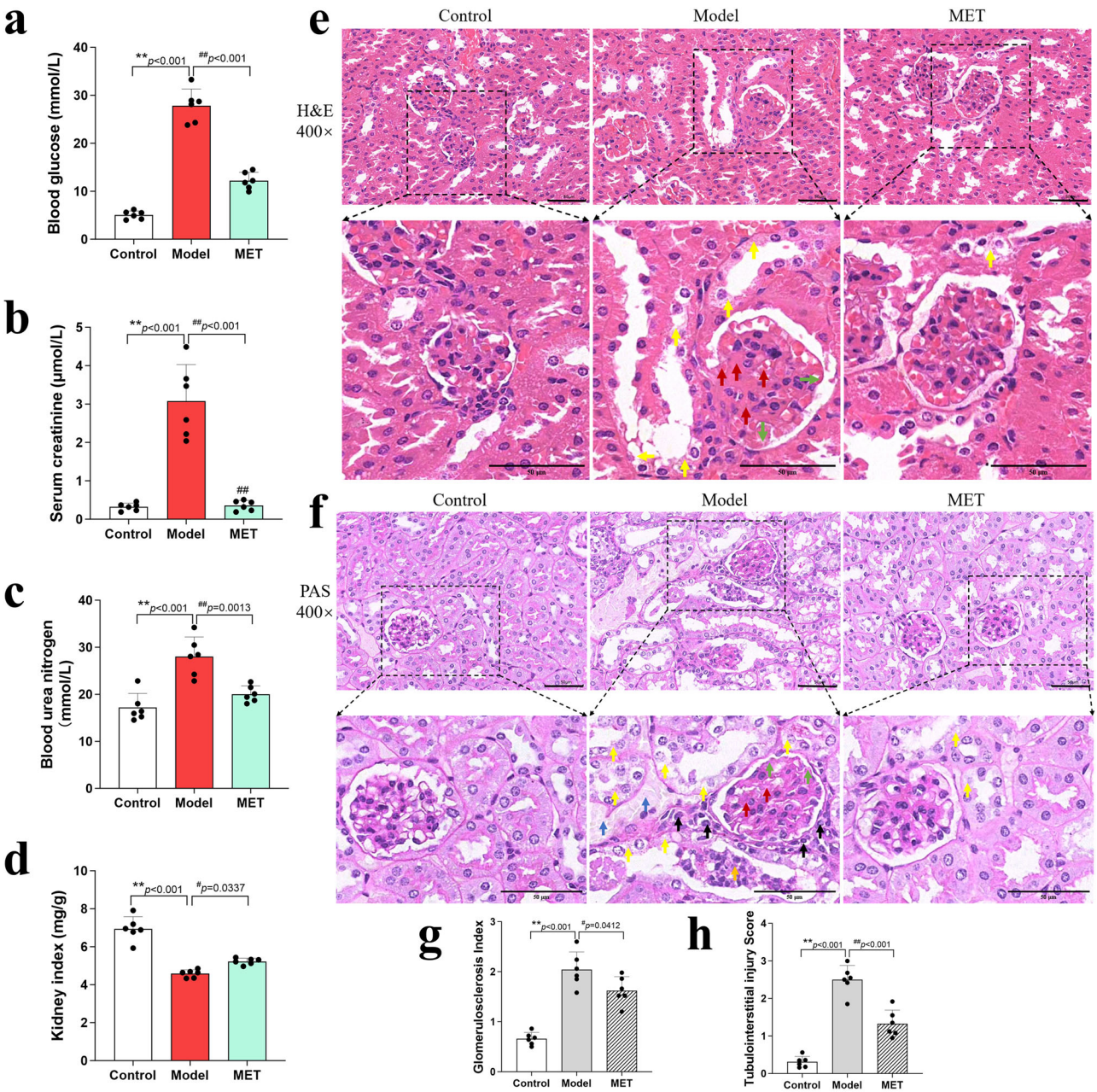

Fig. 1 | Metformin exhibits hypoglycemic and renal protective effects in diabetic kidney disease (DKD). a–d Metformin treatment significantly reduced fasting blood glucose, serum creatinine, and blood urea nitrogen levels, and increased the kidney index in DKD model mice ($n = 6$). **e**, **f** Representative kidney sections stained with hematoxylin and eosin (H&E) and periodic acid-Schiff (PAS) from control, DKD model, and metformin treatment mice (original magnification ×400; scale bar = 50 μm). Arrows indicate characteristic pathological alterations: glycogen and collagen deposition (red), thickening of the glomerular basement membrane (green), vacuolar degeneration of tubular epithelial cells with brush border loss (yellow), tubular dilation with proteinaceous material (blue) and casts (orange), inflammatory cell infiltration (black). **g**, **h** Quantitative analysis of the glomerulosclerosis index and the tubulointerstitial injury scores ($n = 6$ mice). $^{*}P < 0.05$ vs. control group, $^{**}P < 0.01$ vs. control group; $^{\#}P < 0.05$ vs. model group, $^{\#\#}P < 0.01$ vs. model group. Statistical analyses: one-way analysis of variance (ANOVA) with Tukey's post hoc test (**a**–**d**, **g**, **h**). Data represent mean ± standard error of the mean (SEM).

Mice in the Model group exhibited characteristic DKD lesions, including pronounced glomerular hypertrophy, mesangial matrix expansion, thickening of the glomerular basement membrane, and vacuolar degeneration of tubular epithelial cells accompanied by brush border loss. Cytoplasmic vacuoles of varying sizes were observed, along with focal tubular epithelial cell degeneration and necrosis, as well as marked tubular dilation.

PAS staining further confirmed these pathological alterations. Compared with the Control group, the Model mice demonstrated substantial glycogen and collagen deposition, thickening of the glomerular basement membranes, vacuolar degeneration of tubular epithelial cells, tubular dilation, presence of casts and proteinaceous material within the lumen, expansion of the interstitial compartment, and inflammatory cell infiltration. Both the glomerulosclerosis index and tubulointerstitial injury score were significantly higher in the Model group compared to the Control group ($P < 0.001$, Fig. 1g, h). Metformin treatment ameliorated both glomerular injury ($P = 0.0412$) and tubular damage ($P < 0.001$) to varying extents, supporting that metformin exerts renoprotective effects in the DKD mouse model.

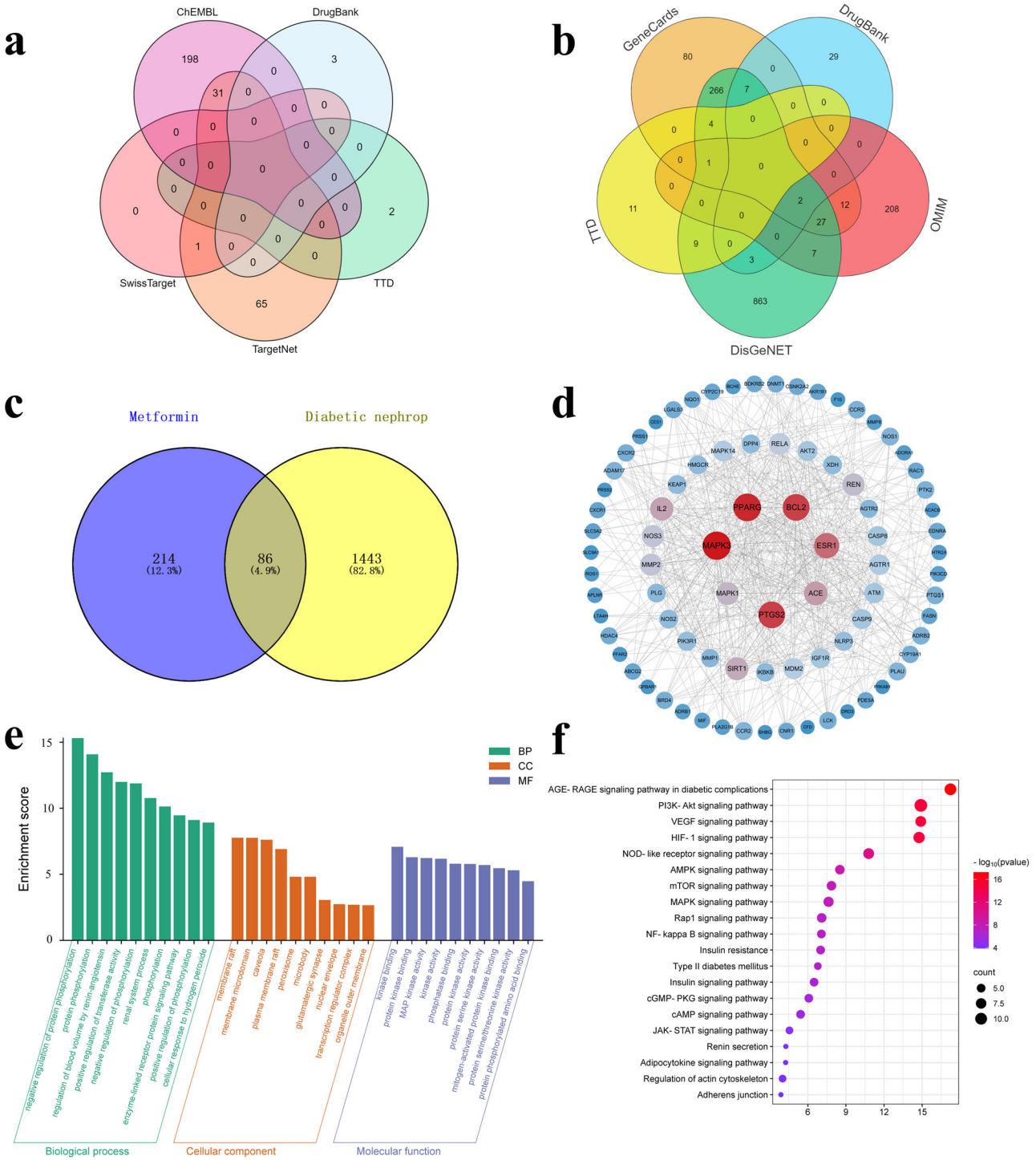

Fig. 2 | Network pharmacology analysis of metformin in diabetic kidney disease (DKD). a Compound targets for metformin obtained from SwissTarget, ChEMBL, DrugBank, Therapeutic Target Database (TTD), and TargetNet databases. **b** DKD disease targets predicted from TTD, GeneCards, DrugBank, Online Mendelian Inheritance in Man (OMIM), and DisGeNET databases. **c** Venn diagram of intersection targets between metformin and DKD. **d** Protein-protein interactions (PPI) network of 83 common targets between metformin and DKD. Circles represent targets, with size and color indicating target importance, from dark blue (less important) to deep red (more important), and larger circles reflecting higher degrees of connectivity. The seven largest and reddest circles in the center correspond to the core targets for metformin treatment of DKD, which were identified based on degree, betweenness, and closeness centrality. **e** Gene Ontology (GO) enrichment analysis of potential targets for metformin in DKD (top 10). **f** Kyoto Encyclopedia of Genes and Genomes (KEGG) enrichment analysis of potential targets for metformin in DKD (top 20). Statistical analyses: Fisher's exact test (**f**).

Target screening and enrichment analysis of metformin on DKD by network pharmacology

A total of 300 targets for metformin were identified from the SwissTarget, TargetNet, TTD, DrugBank, and ChEMBL databases (Fig. 2a). Additionally, 1529 DKD-associated targets were retrieved from the OMIM, DrugBank, GeneCards, TTD, and DisGeNET databases (Fig. 2b). Interaction mapping between metformin targets and DKD-related targets revealed 86 potential therapeutic targets for metformin in DKD (Fig. 2c). The

common targets between metformin and DKD were analyzed using Cytoscape software to construct a PPI network (Fig. 2d). Thirty-two targets with a degree greater than the average were identified as potential targets for metformin in DKD treatment (Supplementary Table 1). Topological analysis identified seven core targets based on degree, betweenness centrality, and closeness centrality: MAPK3, PPARG, PTGS2, BCL2, ESR1, ACE, and MAPK1 (Fig. 2d, Supplementary Table 2).

GO enrichment analysis of the 32 targets indicated that metformin mainly affects the negative regulation of protein phosphorylation (BP: Biological Processes), membrane raft and membrane microdomain (CC: Cellular Components), and protein kinase binding and MAP kinase activity (MF: Molecular Functions) (Fig. 2e). These results suggest that metformin's therapeutic effects in DKD are closely related to the regulation of protein phosphorylation and protein kinase activity. KEGG pathway enrichment analysis further revealed that metformin exerts therapeutic effects in DKD through multiple pathways. The top 20 KEGG pathways include the AGE-RAGE signaling pathway in diabetic complications, PI3K-Akt signaling pathway, VEGF signaling pathway, HIF-1 signaling pathway, AMPK signaling pathway, and MAPK signaling pathway (Fig. 2f).

Phosphoproteomic characterization of metformin for DKD

Using 4D-FastDIA quantitative phosphorylation modification proteomics, we identified 48 phosphorylated proteins and 190 modification sites in the kidney tissues of the model and metformin-treated mice. Principal component analysis (PCA) (Fig. 3a, b), partial least squares-discriminant analysis (PLS-DA) (Supplementary Fig. 1a, b), and orthogonal partial least squares-discriminant analysis (OPLS-DA) (Supplementary Fig. 1c, d) showed significant differences in protein expression between the two groups, indicating metformin's regulatory effect on phosphorylated proteins in DKD.

Differentially phosphorylated proteins and modification sites were identified with $P < 0.05$ and fold change (FC) > 1.5 or < 0.67[25] (Fig. 3c). Visualization through volcano plots (Fig. 3d, g), heatmaps (Fig. 3f, Supplementary Fig. 1e), and radar chart (Fig. 3i) revealed a total of 19 differentially phosphorylated proteins in the metformin group compared to the model group, with 11 upregulated and 8 downregulated proteins. The top 5 upregulated proteins were Pdha1, Map2k2, Map2k1, H3-5, and Pgm3, while the top 5 downregulated proteins were Pkm, Raf1, Mtmr3, Ptk2, and Stk3 (Fig. 3e). The top 5 upregulated and downregulated sites were H3-5_Y100, Ank3_S935, Pdha1_Y289, Map2k2_S306, Map2k1_T386, and Pkm_S77, Raf1_S621, Mtmr3_S633, Ank3_S873, Tmem51_S230, respectively (Fig. 3h).

Functional classification and enrichment analysis of differentially phosphorylated proteins were performed. GO classification (Fig. 4a) showed that at the BP level, differential proteins were mainly related to phosphorylation and MAPK cascade; at the MF level, they primarily affected kinase activity; and at the CC level, they were mainly localized to focal adhesion and cell-substrate junction. Subcellular structure analysis (Fig. 4b) and KEGG annotation (Fig. 4c) indicated that differentially phosphorylated proteins were mainly localized in the cytoplasm and closely related to carbohydrate metabolism. KEGG pathway enrichment analysis using chord plots (Fig. 4d) showed that metformin's treatment of DKD was closely associated with the MAPK signaling pathway, with MAP2K2_S306, MAP2K1_T386, RAF1_S621, and HRAS_S177 being the most significantly phosphorylated proteins and sites.

Metabolomics characterization of blood and urine in patients with DKD

UPLC-MS/MS targeted metabolomics was utilized to analyze serum and urine samples from DKD patients and healthy controls, focusing on carbohydrate metabolism. PCA, PLS-DA, and OPLS-DA analyses demonstrated significant separation in carbohydrate metabolic profiles between the two groups (Fig. 5a–f, Fig. 6a–f). The quality of the OPLS-DA model was assessed using R2Y and Q2 parameters through permutation testing, indicating high stability and reliability with values of 0.998 and 0.969 for blood metabolites, and 0.991 and 0.881 for urine metabolites, respectively.

The variable importance for the projection (VIP) value was employed to assess the influence and interpretative significance of metabolite differences in the classification and discrimination of sample groups. When VIP > 1, it indicates that the corresponding variable significantly contributes to the model, making it a useful criterion for identifying potential biomarkers. With $P < 0.05$, VIP > 1, and FC > 1.5 or < 0.67 as identification conditions, 16 blood differential metabolites were identified by visualizing using volcano plots and heatmaps (Fig. 5g–i, Supplementary Table 4), among which 10 metabolites were upregulated such as Mannitol, Ribose 1-phosphate, D-Xylose, D-Ribose 5-phosphate, L-Glutamic acid, D-Glucuronic acid, Itaconate, D-Arabitol, (R)−3-Hydroxybutyric acid and D-Mannose, and 6 metabolites were downregulated such as Gluconolactone, Oxoglutaric acid, Glyceric acid, 2-Hydroxybutyric acid, 2-Ketobutyric acid, and Galactaric acid. Differential metabolites were analyzed by the KEGG metabolic pathway using $P < 0.05$ and impact > 0.1 as the screening criteria, and the results suggested that DKD was mainly associated with Proximal tubule bicarbonate reclamation, Glyoxylate and dicarboxylate metabolism, ABC transporters and Alanine, aspartate and glutamate metabolism (Fig. 5j). While there were 14 differential urine metabolites (Fig. 6g–i, Supplementary Table 5), among which 9 metabolites such as L-malic acid, 1-keto-D-chiro-inositol, mannitol, L-glutamine, D-arabitol, D-mannose, D-xylose, ribose 1,5-bisphosphate, and galactaric acid were upregulated, and 5 metabolites such as itaconic acid, citric acid, sorbitol, 2-dehydro-3-deoxy-D-glucarate, and glucose 6-phosphate were downregulated. They were mainly associated with pathways such as fructose and mannose metabolism, proximal tubule bicarbonate reclamation, citrate cycle (TCA cycle), and alanine, aspartate, and glutamate metabolism (Fig. 6j).

Metformin regulates blood metabolome in DKD mice

To verify the trend of carbohydrate metabolic profiles in DKD patients and to investigate the effect of metformin treatment on carbohydrate metabolism, we analyzed mouse serum samples using UPLC-MS/MS targeted metabolomics technology. Multivariate statistical analysis (PCA, PLS-DA, OPLS-DA) showed clear separation in metabolic profiles among control, model, and metformin groups (Fig. 7a–c, Supplementary Fig. 2a, b), suggesting that metformin can regulate blood metabolism of DKD. The OPLS-DA permutation test indicated a stable DKD model (R2Y = 0.994, Q2 = 0.913) and potential therapeutic effects of metformin (R2Y = 0.999, Q2 = 0.792).

With VIP > 1, $P < 0.05$, and FC > 1.5 or < 0.67 as identification conditions, the top 10 metabolites were highlighted by the VIP plot in model vs. control and metformin vs. model, respectively (Fig. 7d). Eight metabolites changed significantly in the model group compared to controls, with D-Xylose and Oxalacetic acid upregulated, and Galactitol, D-Glucuronic Acid, L-Ribulose, (2 R)−2-Hydroxy-3-(phosphonatooxy) propanoate, D-Fructose and L-Glutamine downregulated (Fig. 7e, f, Supplementary Table 6). Using $P < 0.05$ and impact > 0.1 as the screening criteria, the KEGG pathway analysis associated DKD with metabolic pathways like Proximal tubule bicarbonate reclamation, Carbon fixation in photosynthetic organisms, and Alanine, aspartate and glutamate metabolism (Supplementary Fig. 2e).

In the metformin group, 10 differential metabolites (Fig. 7e, f, Supplementary Table 7) were identified compared to the model group, including upregulation of L-Malic acid, Alpha-Lactose, D-Glucuronic Acid, Sorbitol, D-Mannose, and L-Glutamic acid, and downregulation of D-Xylose, Oxalacetic acid, Maleic acid, and Methylmalonic acid. These differential metabolites were linked to metabolic pathways such as Proximal tubule bicarbonate reclamation and Alanine, aspartate, and glutamate metabolism (Fig. 7g).

Combined analysis of network pharmacology, phosphoproteomics, and metabolomics

To further elucidate the mechanism of metformin in treating DKD, we conducted KEGG enrichment analysis on 19 differential proteins identified through phosphoproteomics and 86 core targets identified through network

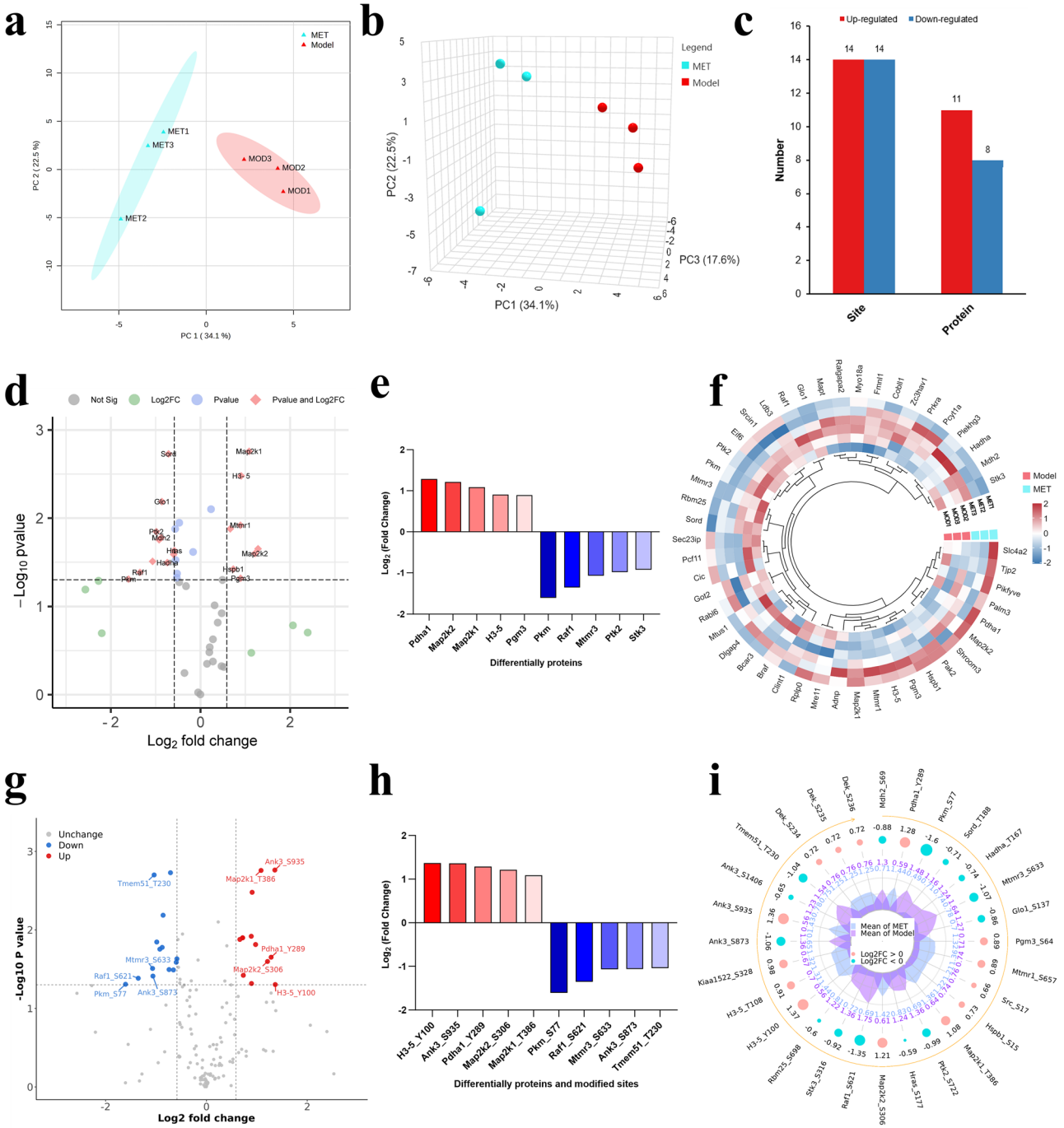

Fig. 3 | Differentially phosphorylated proteins and modification sites in the kidney tissues between diabetic kidney disease (DKD) model and metformin group mice. a Principal component analysis (PCA) 2D score plot of phosphorylated proteins in the model and metformin groups. **b** PCA 3D score plot of phosphorylated proteins in the model and metformin groups. **c** Statistical histogram of differentially phosphorylated proteins and modified sites in the model and metformin group mice. **d** Volcano plot of differentially phosphorylated proteins in the model and metformin groups. Each dot represents a protein. Pink indicates $P < 0.05$ and fold change (FC) > 1.5 or < 0.67, green indicates FC > 1.5 or <0.67 only, blue indicates $P < 0.05$ only. **e** Top 5 differentially phosphorylated proteins in the model and metformin groups identified according to FC when $P < 0.05$. Red represents up-regulated proteins, and blue represents down-regulated proteins. **f** Circular heatmap of differentially phosphorylated proteins in the model and metformin groups. Red squares indicate upregulation and blue squares indicate downregulation. **g** Volcano plot of differentially phosphorylated proteins and modification sites in the model and metformin groups. Each dot represents a protein, red represents up-regulation, and blue represents down-regulation. **h** Top 5 differentially phosphorylated proteins and modification sites in the model and metformin groups identified according to FC and $P < 0.05$. Red represents up-regulation, and blue represents down-regulation. **i** Radar chart of differentially phosphorylated proteins and modification sites in the model and metformin groups. Statistical analyses: two-tailed *t* test (**d**, **g**).

pharmacology. Sankey plot visualization revealed that the MAPK signaling pathway was the most significantly enriched KEGG pathway (smallest *P*-value), with MAPK1 and MAPK3 as the most strongly associated proteins. These findings suggest that metformin treatment of DKD may involve the MAPK signaling pathway, with MAPK1 and MAPK3 as potential therapeutic targets (Fig. 8a).

The literature review suggested that MAPK1 and MAPK3 are closely related to DKD. Molecular docking with metformin was performed using

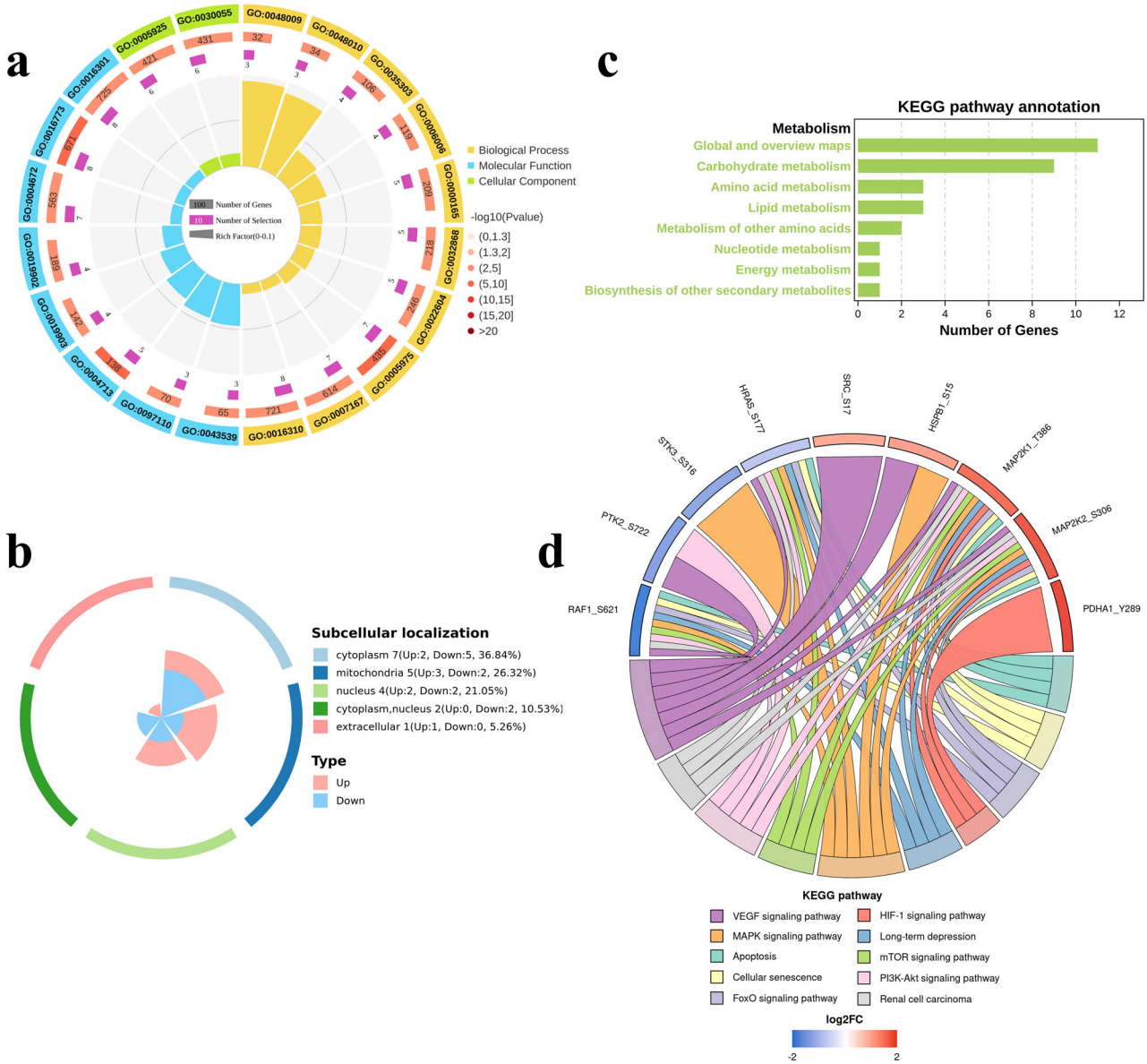

Fig. 4 | Functional classification and enrichment analysis of differentially phosphorylated proteins and modified sites in the kidney tissues between diabetic kidney disease (DKD) model and metformin group mice. a Gene Ontology (GO) enrichment analysis of differentially phosphorylated proteins in the model and metformin groups. From outside to inside, the first circle indicates the GO classification, yellow for biological process, blue for molecular function, and green for cellular component; the second circle represents the number and the *P* value of background proteins in this classification, the more proteins the longer the bar and the smaller the *P* value the redder the color; the third circle represents the number of differential proteins; and the fourth circle represents the Rich Factor value in each GO classification. **b** Subcellular localization annotation of differentially phosphorylated proteins in the model and metformin groups. The outer ring color represents different subcellular structures, while the inner ring shows upregulated proteins in pink and downregulated proteins in blue. **c** Kyoto Encyclopedia of Genes and Genomes (KEGG) pathway annotation for differentially phosphorylated proteins in the model and metformin groups. **d** KEGG enrichment chord plot of differentially phosphorylated proteins and sites. Red represents up-regulation, blue represents down-regulation, and the larger the fold change (FC) the darker the color.

the CB-DOCK2 online software. The binding energies of MAPK1 and MAPK3 to metformin were −5.3 kcal/mol and −5.6 kcal/mol, respectively, indicating good binding affinity. Molecular docking visualization results are shown in Fig. 8b, c.

In the blood and urine samples from clinical subjects, Mannitol, D-Arabitol, D-Mannose, and D-Xylose showed consistent changes and were associated with DKD risk. The main metabolic pathways involved were Proximal tubule bicarbonate reclamation and Alanine, aspartate and glutamate metabolism. In mouse blood samples, three common metabolites—D-Xylose, Oxalacetic acid, and D-Glucuronic acid—exhibited significant changes after metformin treatment, with the involved metabolic pathways related to Proximal tubule bicarbonate reclamation and Alanine, aspartate and glutamate metabolism.

Using a Venn plot (Fig. 8d), we were surprised to discover that D-Xylose showed a consistent trend in both clinical subjects and mouse samples, suggesting its potential as a biomarker for metformin treatment of DKD. The potential metabolic pathways were Proximal tubule bicarbonate reclamation and alanine, aspartate and glutamate metabolism (Fig. 8e).

Discussion

DKD is a chronic kidney disease caused by DM, where prolonged hyperglycemia causes kidney damage, contributing to increased all-cause and cardiovascular mortality[26]. With the rising prevalence of DM, DKD has also

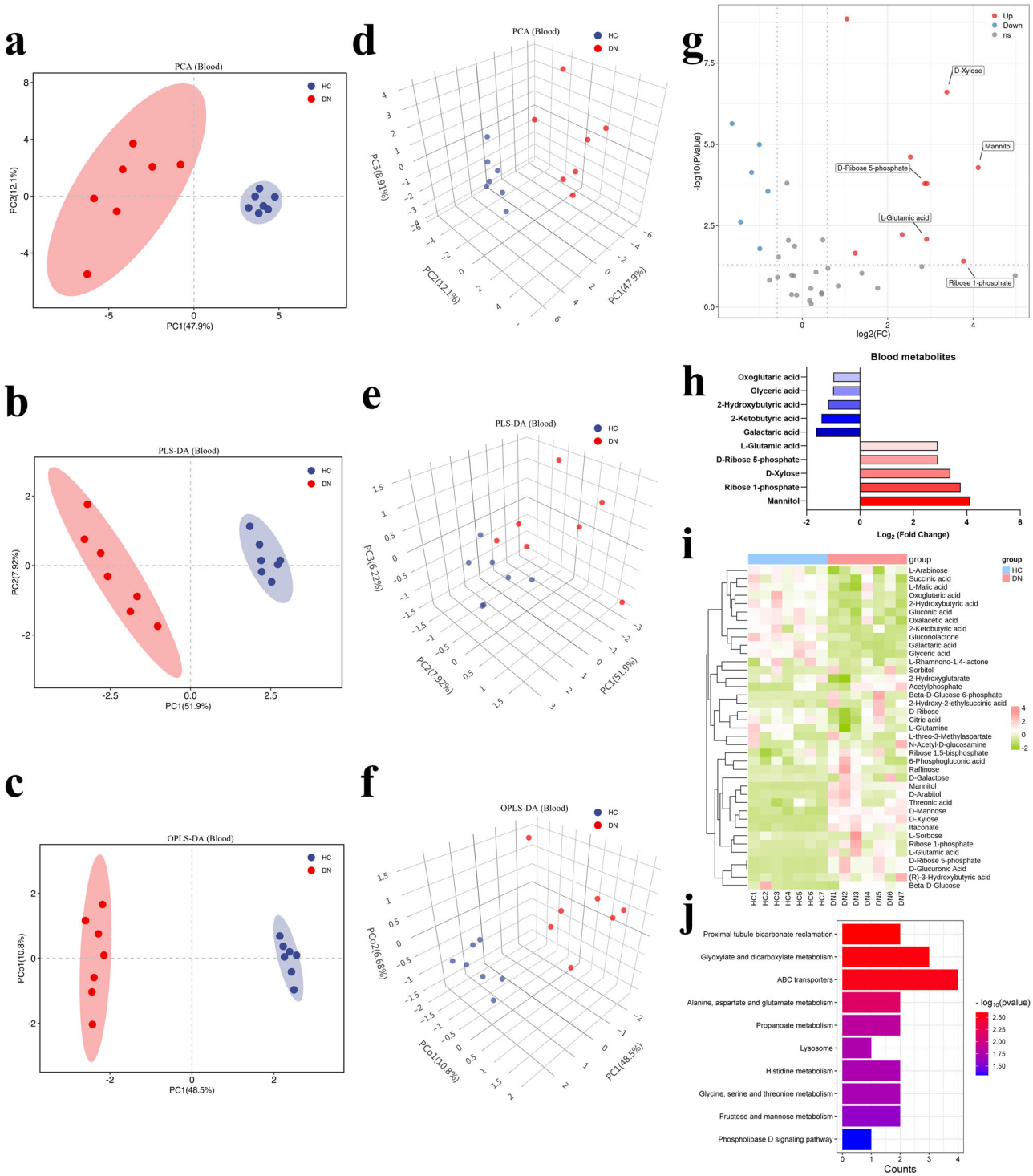

Fig. 5 | Characteristics of carbohydrate metabolites in blood from diabetic kidney disease (DKD) patients and healthy controls. a–f Multivariate statistical analysis of carbohydrate metabolism in DKD patients and healthy controls: **a** Principal component analysis (PCA) 2D score plot; **b** Partial least squares-discriminant analysis (PLS-DA) 2D score plot; **c** Orthogonal partial least squares-discriminant analysis (OPLS-DA) 2D score plot; **d** PCA 3D score plot; **e** PLS-DA 3D score plot; **f** OPLS-DA 3D score plot. Each dot represents a subject, with blue indicating healthy controls (HC) and red indicating DKD patients (DN). **g** Volcano plot of differential metabolites in DKD patients and healthy controls. Each dot represents a metabolite, red represents up-regulation, and blue represents down-regulation. **h** Top 5 differential metabolites in the DKD patients and healthy controls identified according to fold change and $P < 0.05$. Red represents up-regulation, and blue represents down-regulation. **i** Heatmap of differential metabolites in the DKD patients and healthy controls. Pink squares indicate upregulation and olive squares indicate downregulation. **j** Kyoto Encyclopedia of Genes and Genomes (KEGG) metabolic pathway analysis of differential metabolites in the DKD patients and healthy controls. Statistical analyses: two-tailed *t* test (**g**) and Fisher's exact test (**j**).

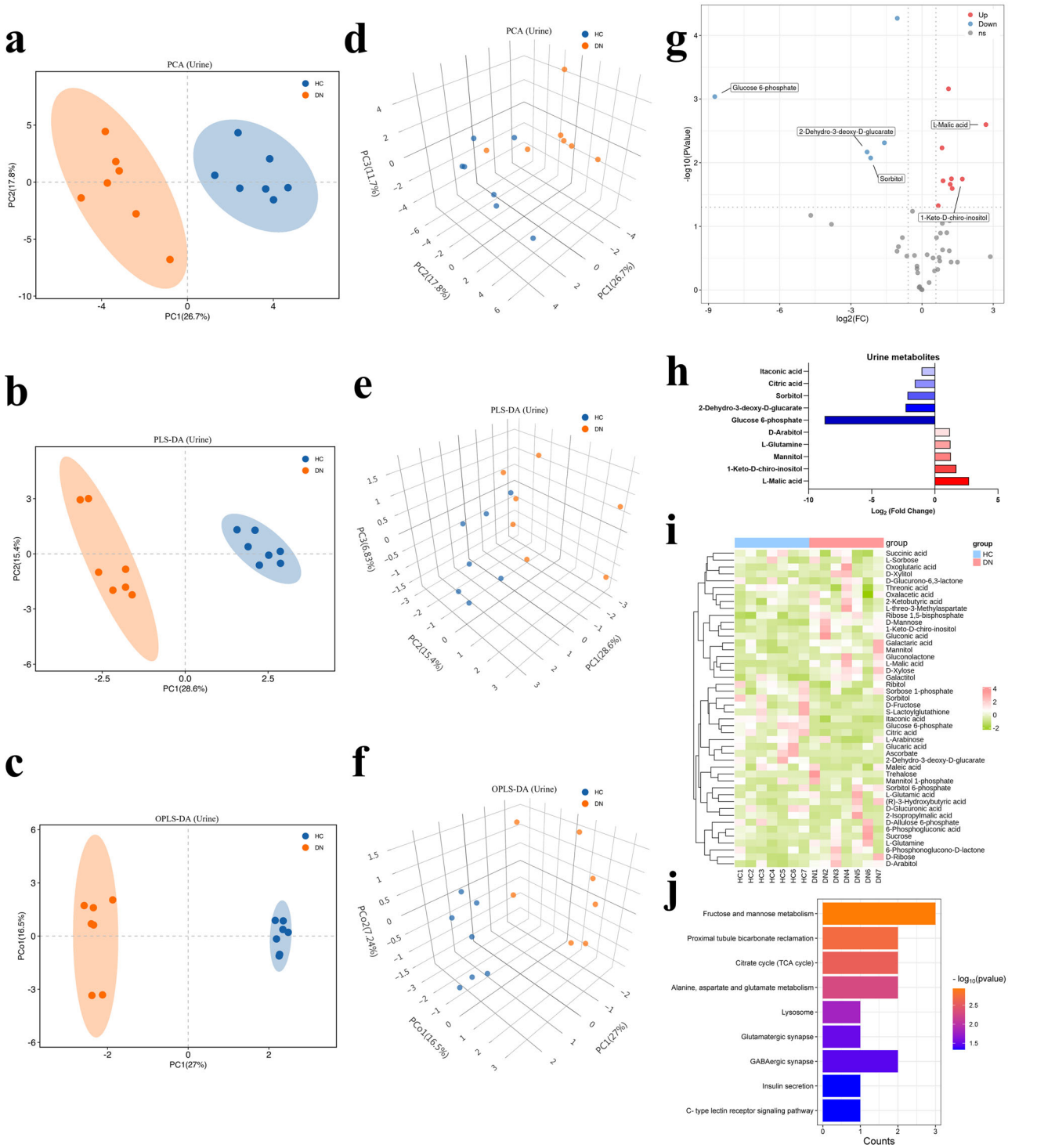

Fig. 6 | Characteristics of carbohydrate metabolites in urine from diabetic kidney disease (DKD) patients and healthy controls. a–f Multivariate statistical analysis of carbohydrate metabolism in DKD patients and healthy controls: **a** Principal component analysis (PCA) 2D score plot; **b** Partial least squares-discriminant analysis (PLS-DA) 2D score plot; **c** Orthogonal partial least squares-discriminant analysis (OPLS-DA) 2D score plot; **d** PCA 3D score plot; **e** PLS-DA 3D score plot; **f** OPLS-DA 3D score plot. Each dot represents a subject, with blue indicating healthy controls (HC) and red indicating DKD patients (DN). **g** Volcano plot of differential metabolites in DKD patients and healthy controls. Each dot represents a metabolite, red represents up-regulation, and blue represents down-regulation. **h** Top 5 differential metabolites in the DKD patients and healthy controls identified according to fold change and $P < 0.05$. Red represents up-regulation, and blue represents down-regulation. **i** Heatmap of differential metabolites in the DKD patients and healthy controls. Pink squares indicate upregulation and olive squares indicate downregulation. **j** Kyoto Encyclopedia of Genes and Genomes (KEGG) metabolic pathway analysis of differential metabolites in the DKD patients and healthy controls. Statistical analyses: two-tailed *t* test (**g**) and Fisher's exact test (**j**).

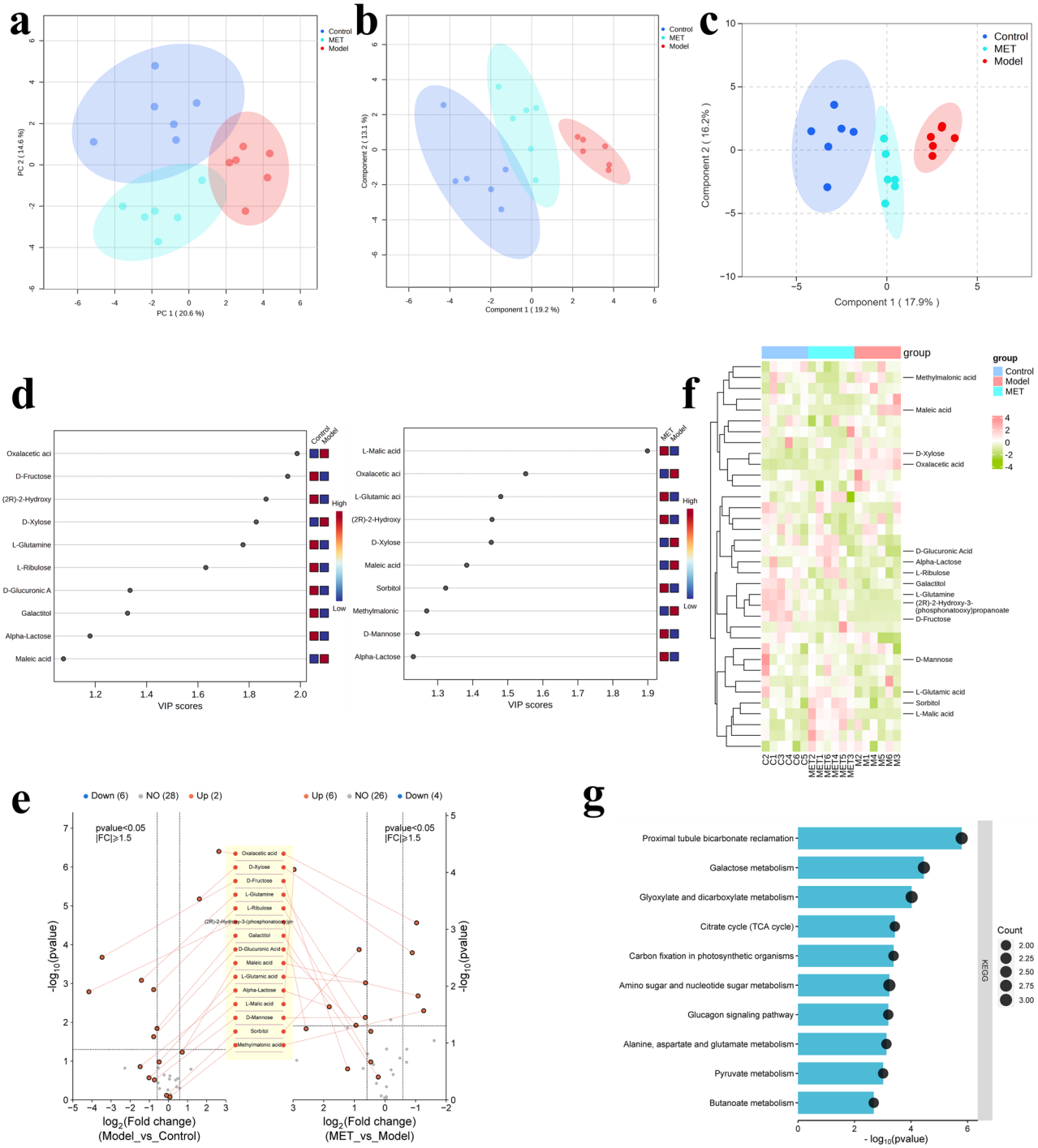

Fig. 7 | Profiling of carbohydrate metabolites in serum from diabetic kidney disease (DKD) model mice. a–c Principal component analysis (PCA), Partial least squares-discriminant analysis (PLS-DA), and Orthogonal partial least squares-discriminant analysis (OPLS-DA) score plots among the control, model, and metformin treatment groups. **d** The variable importance for the projection (VIP) score plots illustrating the differences between the control and model groups, and between the model and metformin treatment groups. **e** Volcano plots depicting differential metabolites between the control, model, and metformin groups. Each dot represents a metabolite, with blue denoting downregulation and red denoting upregulation; left panel shows model vs control, while right panel shows metformin vs model comparison. **f** Heatmap displaying the differential expression of metabolites across the control, model and metformin groups. Pink squares indicate upregulation and olive squares indicate downregulation. **g** Kyoto Encyclopedia of Genes and Genomes (KEGG) metabolic pathway analysis of differential metabolites between the model and metformin groups. The smaller the *P* value the longer the bar and the more metabolites in the pathway the larger the dot. Statistical analyses: two-tailed *t* test (**e**) and Fisher's exact test (**g**).

become a significant global public health challenge[26,27], being a leading cause of CKD and ESRD worldwide[28,29]. Effective DKD treatment emphasizes early intervention and comprehensive management, including lifestyle adjustment and control of blood glucose, blood pressure, and lipids. Blood glucose control is particularly crucial, as it significantly affects the onset and progression of DKD. Early control can delay urinary protein increase and renal function decline in DM patients[30], for instance, a 40% increase in the risk of microalbuminuria is associated with a 10% decrease in time in range (TIR), which reflects blood glucose fluctuation[31]. Metformin, a primary antidiabetic drug for T2DM, is excreted unchanged in the urine and has

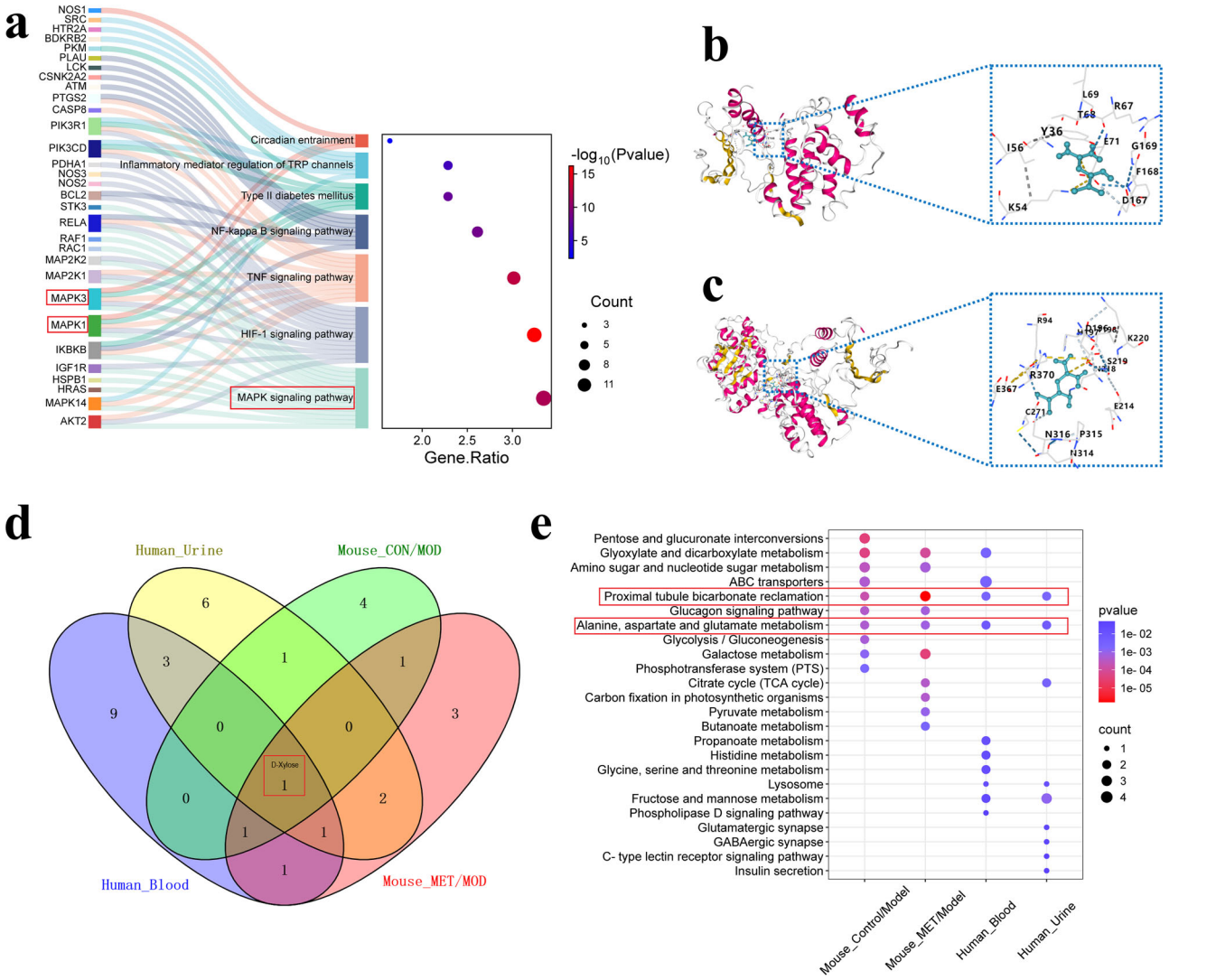

Fig. 8 | Combined analysis of network pharmacology, phosphoproteomics, and metabolomics. a Potential targets and Kyoto Encyclopedia of Genes and Genomes (KEGG) pathways for metformin treatment of diabetic kidney disease (DKD). The left panel presents a Sankey diagram illustrating enriched KEGG pathways and associated proteins, with bar lengths reflecting enrichment levels; the right panel is a dot plot, where dot size indicates the number of background proteins in the pathway, and color represents the *P* value, with redder dots indicating smaller *P*-values. Molecular docking of metformin with MAPK1 (**b**) and MAPK3 (**c**). **d** The common metabolites observed in the Human_Blood, Human_Urine, Mouse_Control/Model, and Mouse_Met/Model. **e** The metabolic pathways observed in the Human_Blood, Human_Urine, Mouse_Control/Model, and Mouse_Met/Model. Statistical analyses: Fisher's exact test (**a**, **e**).

been shown in several clinical studies, including the United Kingdom Prospective Diabetes Study, to reduce all-cause mortality and slow ESRD progression in patients with T2DM and DKD[5,6,32,33]. Both in vitro and in vivo experiments also suggest metformin's beneficial effects on the kidney[34].

This study confirmed metformin's hypoglycemic and renal protective effects on DKD through animal experiments. Network pharmacology, along with GO and KEGG enrichment analyses, predicted potential targets of metformin in DKD treatment, suggesting a mechanism related to protein phosphorylation. Phosphoproteomic analysis of DKD model mice kidneys identified differential proteins and modification sites. Subcellular structure and KEGG annotations indicated that the differentially phosphorylated proteins were primarily located in the cytoplasm and closely associated with carbohydrate metabolism. Blood and urine analysis of DKD patients identified potential biomarkers and metabolic pathways, further validated through blood metabolomics of DKD model mice. Integrating network pharmacology, phosphoproteomics, targeted metabolomics, and molecular docking revealed the following main findings: (1) Metformin effectively reduces FBG, SCr, and BUN levels in DKD model mice; (2) MAPK1 and MAPK3 are potential targets of metformin in DKD treatment, with the MAPK signaling pathway as a potential signaling pathway; (3) Mannitol, D-Arabitol, D-Mannose, and D-Xylose are associated with DKD risk; (4) D-Xylose is a potential biomarker for metformin treatment of DKD, with Proximal tubule bicarbonate reclamation and Alanine, aspartate and glutamate metabolism as potential metabolic pathways.

Metformin has been used clinically for T2DM for over 50 years. In recent years, accumulating evidence has revealed multiple extraglycemic effects, such as anti-inflammatory[35], anti-aging[36], and renal protection[6,33] have been gradually discovered. Zhou et al. found that[37] the expression level of tenascin-C (TNC) in the serum of T2DM patients, DKD rats, and rat mesangial cells stimulated by high glucose increased. Metformin could protect the kidney in DKD by regulating the inflammation and fibrosis process through the TNC/TLR4/NF-κB/miR-155-5p inflammatory loop[37]. Kim et al. found that[38] metformin attenuated endoplasmic reticulum stress and renal fibrosis by decreasing glucose-related protein 78 and phosphorylated eukaryotic initiation factor-2α, possibly related to protein phosphorylation[39]. Our study's findings align with these results, showing metformin's hypoglycemic and renal protective effects in DKD model mice and suggesting a mechanism involving protein phosphorylation.

Proteins execute vital bodily functions, often requiring PTMs like phosphorylation to function properly. Phosphorylation, a well-studied PTM, typically occurs in the nucleus or cytoplasm and dynamically regulates protein phosphorylation and dephosphorylation through kinases and phosphatases[40], influencing processes such as apoptosis, immune response, and cell metabolism, and is closely related to diseases such as tumors and DKD[40]. MAPKs are a group of highly conserved serine/threonine protein kinases that transmit extracellular stimulation signals such as oxidative stress, DNA damage, high glucose, and high osmotic pressure from the cell surface to the interior of the cell nucleus[41]. The MAPK signaling pathway, a crucial pathway in eukaryotic signal transmission, regulates various physiological and pathological processes, including cell proliferation, differentiation, apoptosis, and inflammatory response[42]. MAPKs activate when phosphorylated. Classic MAPKs include extracellular signal-regulated kinase 1/2 (ERK1/2, also known as MAPK3/1), p38 MAPK, c-Jun NH2-terminal kinase (JNK), and ERK5 – four major subfamilies[41]. Correspondingly, MAPK has four classical signal pathways, among which, ERK pathway is the most classical MAPK signal pathway, critical in DKD development. When stimulated by extracellular stimulation signals such as high glucose, Ras is activated, and activated Ras recruits Raf to the plasma membrane, so that its phosphorylation is activated. Activated Raf further binds to MEK1/2 downstream and activates ERK1/2, phosphorylates activated ERK1/2 into the nucleus to initiate gene expression related to cell cycle, proliferation, and adhesion, and plays an important role in the occurrence and development of DKD[43,44]. Osasenaga et al. found that high glucose levels can activate ROS, triggering pathways like p38MAPK and leading to phosphorylation of insulin receptor substrates, ultimately resulting in diabetes[45]. This is consistent with our findings. Through phosphoproteomics analysis and molecular docking, we identified MAPK1 and MAPK3 as potential metformin targets in DKD, with the MAPK signaling pathway being a key enrichment pathway. Upregulated modification sites included Ank3_S935, Pdha1_Y289, Map2k2_S306, and Map2k1_T386, while downregulated sites included Pkm_S77, Raf1_S621, Mtmr3_S633, Ank3_S873, and Tmem51_S230. Additionally, the differentially phosphorylated proteins were primarily localized in the cytoplasm and were closely related to carbohydrate metabolism.

Metabolomics, focusing on small molecule metabolites, observes the dynamic change law of metabolites from the overall level, and can explore disease biomarkers and understand the mechanisms of diseases like DM and its complications[46]. Recent metabolomics studies indicate that DKD patients exhibit multiple biochemical metabolic pathway abnormalities[47]. A study in Singapore analyzed 220 circulating metabolites in 2772 diabetic patients and identified circulating tyrosine as an important factor for detecting DKD, and other metabolites like lactate and citrate have also been linked to DKD[48]. Another large cohort study on the association of plasma metabolites with the risk of ESRD progression in T2DM patients found that tryptophan and kynurenine were involved in the risk of renal progression in T2DM patients, with tryptophan negatively associated with ESRD risk and kynurenine-to-tryptophan ratio positively associated with ESRD risk, with hazard ratios adjusted for clinical risk factors of 0.62, respectively (95% CI: 0.51, 0.75) and 1.48 (95% CI: 1.20, 1.84) per 1 SD[49]. This study's targeted carbohydrate metabolomics analysis from the blood and urine of DKD patients showed that Mannitol, D-Arabitol, D-Mannose, and D-Xylose were associated with DKD risk, with Proximal tubule bicarbonate reclamation and Alanine, aspartate and glutamate metabolism as potential metabolic pathways.

D-Xylose, a functional monosaccharide found widely in plants rich in hemicellulose such as the core of maize straw and *Auricularia auricula*, has various physiological regulation functions and is approved by the Food and Drug Administration, among other regulations, for use as a calorie-free sweetener or sugar substitute. D-Xylose belongs to water-soluble dietary fiber, which can regulate intestinal flora and promote the proliferation of beneficial bacteria such as *Bifidobacterium*[50]. In addition, D-Xylose can block the absorption of bile acids and hydrolysis of carbohydrates, and has invertase and α-amylase inhibitory activity[50]. Early animal experiments showed that adding 10%(w/w) xylose to sucrose drinks inhibited rapid increases in blood glucose and insulin levels in rats[51]. This was confirmed in a randomized controlled trial in South Korea, where blood glucose and serum insulin levels were significantly reduced in hyperglycemic subjects after consumption of sucrose beverages containing xylose compared with control groups, suggesting that D-Xylose is beneficial to postprandial blood glucose control[50]. The beneficial effect of D-Xylose on postprandial blood glucose was also confirmed in an early clinical trial in Australia, where 12 subjects with T2DM were treated with selegiline or placebo, and were given beverages containing either D-Xylose or sucralose (control) after fasting overnight, and it was found that blood glucose was lower than that of the control group after consuming D-Xylose-containing beverages in both groups, with the lowest blood glucose in the sitagliptin group, suggesting that D-Xylose reduces postprandial glucose in T2DM patients and enhances the effect of DDP-4 inhibitors[52]. This study found consistent trends in D-xylose levels in clinical subjects and DKD model mice, suggesting that metformin may regulate D-xylose metabolites to treat DKD, and D-xylose can serve as a potential biomarker for metformin treatment.

This study systematically analyzed blood and urine samples from DKD patients and DKD model mice, integrating network pharmacology, phosphoproteomics, and targeted metabolomics. It confirmed metformin's efficacy in treating DKD and proposed that metformin may act through the MAPK signaling pathway, with D-Xylose as a potential biomarker. However, this study still has some limitations. First, the sample size for human samples in the clinical study is relatively small. Second, while D-Xylose was proposed as a potential biomarker, its precise mechanism in metformin's treatment of DKD remains unclear. Therefore, future studies should increase sample sizes and further investigate the regulatory role of D-Xylose in the context of metformin treatment in DKD, to identify novel therapeutic targets for this condition.

In conclusion, this study confirmed the hypoglycemic and renal protective effects of metformin in DKD using model mice. Network pharmacology and phosphoproteomic analyses identified MAPK1 and MAPK3 as key targets of metformin, with the MAPK signaling pathway in its therapeutic action. Targeted metabolomics revealed associations between Mannitol, D-Arabitol, D-Mannose, D-Xylose, and DKD risk, with D-Xylose highlighted as a potential biomarker for metformin's effects. These findings suggest that metformin's benefits in DKD may involve modulation of the MAPK pathway and D-Xylose metabolism, with proximal tubule bicarbonate reclamation and alanine, aspartate and glutamate metabolism as potential metabolic pathways.

Data availability

The source data underlying the figures presented in this study are provided in the Supplementary Information. Specifically, the source data for Fig. 2d are available in Supplementary Table 2, for Fig. 5 in Supplementary Table 4, for Fig. 6 in Supplementary Table 5, and for Fig. 7 in Supplementary Table 6 and 7. Additional supporting data not included in the Supplementary Information are available from the corresponding author upon reasonable request.

Received: 5 September 2024; Accepted: 12 September 2025;
Published online: 04 November 2025

References

1. Sun, H. et al. IDF Diabetes Atlas: Global, regional and country-level diabetes prevalence estimates for 2021 and projections for 2045. *Diab Res. Clin. Pr.* **183**, 109119 (2022).
2. IDF Diabetes Atlas Reports. https://diabetesatlas.org/atlas/diabetes-and-kidney-disease. (2023)
3. Cheng, H. T., Xu, X., Lim, P. S. & Hung, K. Y. Worldwide Epidemiology of Diabetes-Related End-Stage Renal Disease, 2000-2015. *Diab Care.* **44**, 89–97 (2021).

4. Fan, X. et al. Mitochondrial metabolic reprogramming in diabetic kidney disease. *Cell Death Dis.* **15**, 442 (2024).
5. Crowley, M. J. et al. Clinical outcomes of metformin use in populations with chronic kidney disease, congestive heart failure, or chronic liver disease: A systematic review. *Ann. Intern Med* **166**, 191–200 (2017).
6. Kwon, S. et al. The long-term effects of metformin on patients with type 2 diabetic kidney disease. *Diab Care* **43**, 948–955 (2020).
7. American Diabetes Association. 9. Pharmacologic approaches to glycemic treatment: Standards of medical care in diabetes-2020. *Diab Care* **43**, S98–S110 (2020).
8. de Boer, I. H. et al. Diabetes management in chronic kidney disease: A consensus report by the American Diabetes Association (ADA) and Kidney Disease: Improving Global Outcomes (KDIGO). *Kidney Int* **102**, 974–989 (2022).
9. Rossing, P. et al. Executive summary of the KDIGO 2022 clinical practice guideline for diabetes management in chronic kidney disease: an update based on rapidly emerging new evidence. *Kidney Int.* **102**, 990–999 (2022).
10. Morita, Y. et al. Enhanced release of glucose into the intraluminal space of the intestine associated with metformin treatment as revealed by [(18)F]Fluorodeoxyglucose PET-MRI. *Diab Care* **43**, 1796–1802 (2020).
11. Ma, T. et al. Low-dose metformin targets the lysosomal AMPK pathway through PEN2. *Nature* **603**, 159–165 (2022).
12. Qiu, S. et al. Spatially segregated multiomics decodes metformin-mediated functional-specific metabolic characteristics in diabetic kidney disease. *Life Metab* https://doi.org/10.1093/lifemeta/loaf019 (2025).
13. Ruiz-Mitjana, A. et al. Metformin exhibits antineoplastic effects on Pten-deficient endometrial cancer by interfering with TGF-β and p38/ERK MAPK signalling. *Biomed. Pharmacother.* **168**, 115817 (2023).
14. Lin, C. et al. Metabolomics for clinical biomarker discovery and therapeutic target identification. *Molecules* **29**, 2198 (2025).
15. Qiu, S. et al. Small molecule metabolites: Discovery of biomarkers and therapeutic targets. *Signal Transduct. Target Ther.* **8**, 132 (2023).
16. Kurgan, N., Kjærgaard Larsen, J. & Deshmukh, A. S. Harnessing the power of proteomics in precision diabetes medicine. *Diabetologia* **67**, 783–797 (2024).
17. Lee, J. M., Hammarén, H. M., Savitski, M. M. & Baek, S. H. Control of protein stability by post-translational modifications. *Nat. Commun.* **14**, 201 (2023).
18. Needham, E. J., Parker, B. L., Burykin, T., James, D. E. & Humphrey, S. J. Illuminating the dark phosphoproteome. *Sci. Signal* **12**, eaau8645 (2019).
19. Fazakerley, D. J. et al. Phosphoproteomics reveals rewiring of the insulin signaling network and multi-nodal defects in insulin resistance. *Nat. Commun.* **14**, 923 (2023).
20. Jiang, L. et al. METTL3-mediated m6A modification of TIMP2 mRNA promotes podocyte injury in diabetic nephropathy. *Mol. Ther.* **30**, 1721–1740 (2022).
21. Zhu, Y. et al. Necroptosis mediated by receptor interaction protein kinase 1 and 3 aggravates chronic kidney injury of subtotal nephrectomised rats. *Biochem Biophys. Res Commun.* **461**, 575–581 (2015).
22. Han, Y. C. et al. AMPK agonist alleviate renal tubulointerstitial fibrosis via activating mitophagy in high fat and streptozotocin induced diabetic mice. *Cell Death Dis.* **12**, 925 (2021).
23. Chen, H. et al. VDR regulates mitochondrial function as a protective mechanism against renal tubular cell injury in diabetic rats. *Redox Biol.* **70**, 103062 (2024).
24. Qiu S. et al. Comprehensive multiomics revealed astragaloside IV regulating carbohydrate metabolism dysfunction through clinical, animal and cellular platforms. *Food Biosci*. https://doi.org/10.1016/j.fbio.2025.106757. (2025).
25. Yang, X. et al. Proteomics and β-hydroxybutyrylation modification characterization in the hearts of naturally senescent mice. *Mol. Cell Proteom.* **22**, 100659 (2023).
26. GBD Chronic Kidney Disease Collaboration. Global, regional, and national burden of chronic kidney disease, 1990-2017: A systematic analysis for the Global Burden of Disease Study 2017. *Lancet* **395**, 709–733 (2020).
27. Xie, Y. et al. Analysis of the Global Burden of Disease study highlights the global, regional, and national trends of chronic kidney disease epidemiology from 1990 to 2016. *Kidney Int.* **94**, 567–581 (2018).
28. Pan, X. et al. The burden of diabetes-related chronic kidney disease in China From 1990 to 2019. *Front Endocrinol. (Lausanne)* **13**, 892860 (2022).
29. Gupta, S., Dominguez, M. & Golestaneh, L. Diabetic kidney disease: An update. *Med Clin. North Am.* **107**, 689–705 (2023).
30. Agrawal, L. et al. Long-term follow-up of intensive glycaemic control on renal outcomes in the Veterans Affairs Diabetes Trial (VADT). *Diabetologia* **61**, 295–299 (2018).
31. Beck, R. W. et al. Validation of time in range as an outcome measure for diabetes clinical trials. *Diab Care* **42**, 400–405 (2019).
32. Holman, R. R., Paul, S. K., Bethel, M. A., Matthews, D. R. & Neil, H. A. 10-year follow-up of intensive glucose control in type 2 diabetes. *N. Engl. J. Med*. **359**, 1577–1589 (2008).
33. Charytan, D. M. et al. Metformin use and cardiovascular events in patients with type 2 diabetes and chronic kidney disease. *Diab Obes. Metab.* **21**, 1199–1208 (2019).
34. Song, A., Zhang, C. & Meng, X. Mechanism and application of metformin in kidney diseases: An update. *Biomed. Pharmacother.* **138**, 111454 (2021).
35. Chai, J. et al. Proteomics exploration of metformin hydrochloride for diabetic kidney disease treatment via the butanoate metabolism pathway. *J. Pharm. Biomed. Anal.* **254**, 116584 (2025).
36. Fang, J. et al. Metformin alleviates human cellular aging by upregulating the endoplasmic reticulum glutathione peroxidase 7. *Aging Cell* **17**, e12765 (2018).
37. Zhou, Y. et al. Metformin regulates inflammation and fibrosis in diabetic kidney disease through TNC/TLR4/NF-κB/miR-155-5p inflammatory loop. *World J. Diab* **12**, 19–46 (2021).
38. Kim, H. et al. Activation of AMP-activated protein kinase inhibits ER stress and renal fibrosis. *Am. J. Physiol. Ren. Physiol.* **308**, F226–F236 (2015).
39. Lee, M. et al. Phosphorylation of acetyl-CoA Carboxylase by AMPK reduces renal fibrosis and is essential for the anti-fibrotic effect of metformin. *J. Am. Soc. Nephrol.* **29**, 2326–2336 (2018).
40. Wu, X. et al. Targeting protein modifications in metabolic diseases: molecular mechanisms and targeted therapies. *Signal Transduct. Target Ther.* **8**, 220 (2023).
41. Kassouf, T. & Sumara, G. Impact of conventional and atypical MAPKs on the development of metabolic diseases. *Biomolecules* **10**, 1256 (2020).
42. Ng, G. Y. Q. et al. Role of mitogen-activated protein (MAP) kinase pathways in metabolic diseases. *Genome Integr.* **15**, e20230003 (2024).
43. Yuan, N. et al. Targeting ROCK1 in diabetic kidney disease: Unraveling mesangial fibrosis mechanisms and introducing myricetin as a novel antagonist. *Biomed. Pharmacother.* **171**, 116208 (2024).
44. Livingston, M. J. et al. Autophagy activates EGR1 via MAPK/ERK to induce FGF2 in renal tubular cells for fibroblast activation and fibrosis during maladaptive kidney repair. *Autophagy* **20**, 1032–1053 (2024).
45. Ighodaro, O. M. Molecular pathways associated with oxidative stress in diabetes mellitus. *Biomed. Pharmacother.* **108**, 656–662 (2018).
46. Kikuchi, K. et al. Gut microbiome-derived phenyl sulfate contributes to albuminuria in diabetic kidney disease. *Nat. Commun.* **10**, 1835 (2019).

47. Li, H. et al. Global status and trends of metabolomics in diabetes: A literature visualization knowledge graph study. *World J. Diab* **15**, 1021–1044 (2024).
48. He, F. et al. Development and External Validation of Machine Learning Models for Diabetic Microvascular Complications: Cross-Sectional Study With Metabolites. *J. Med Internet Res* **26**, e41065 (2024).
49. Liu, J. J. et al. Plasma tryptophan-kynurenine pathway metabolites and risk for progression to end-stage kidney disease in patients with type 2 diabetes. *Diab Care* **46**, 2223–2231 (2023).
50. Jun, Y. J. et al. Beneficial effect of xylose consumption on postprandial hyperglycemia in Korean: a randomized double-blind, crossover design. *Trials* **17**, 139 (2016).
51. Asano, T., Yoshimura, Y. & Kunugita, K. J. N. E. S. G. Sucrase inhibitory activity of D-Xylose and effect on the elevation of blood glucose in rats. *Nippon Eiyo Shokuryo Gakkaishi* **49**, 157–162 (1996).
52. Wu, T. et al. Effects of a D-xylose preload with or without sitagliptin on gastric emptying, glucagon-like peptide-1, and postprandial glycemia in type 2 diabetes. *Diab Care* **36**, 1913–1918 (2013).

Acknowledgements

We are grateful for the generous support from the Program of Natural Science Foundation of State (Grant No. 81973745, 82104733), Hainan Province 'Nanhai New Star' Science and Technology Innovation Talent Platform Project by Hainan Provincial Department of Science and Technology (NHXXRCXM202317), Academic Enhancement Support Program by Hainan Medical University (XSTS2025079), Natural Science Foundation of Heilongjiang Province (YQ2019H030). The authors are grateful to the support and assistance in terms of instruments and facilities provided by Public Research Center of Hainan Medical University.

Author contributions

D.Xie, Y.Zhu, S.Guo, and H.Li conducted the experiments, analyzed the data and wrote the manuscript. Z.Wang, X.Wang, and Y.Cai conducted the experiments, analyzed the data, and wrote the manuscript. J.Chai, Y.Wang, Z.Hu, and S.Wang conducted the experiments and analyzed the data. L.Chen, S.Qiu, Y.Xie, and A.Zhang designed the experiments, analyzed the data, revised the manuscript, and approved the final version.

Competing interests

The authors declare no competing interests.

Additional information

Supplementary information The online version contains supplementary material available at https://doi.org/10.1038/s43856-025-01152-7.

Correspondence and requests for materials should be addressed to Lasi Chen, Shi Qiu, Yiqiang Xie or Aihua Zhang.

Peer review information *Communications Medicine* thanks the anonymous reviewers for their contribution to the peer review of this work.